

Article

# Decreased Photosynthetic Efficiency in Response to Site Translocation and Elevated Temperature Is Mitigated with LPS Exposure in *Porites astreoides* Symbionts

Tyler E. Harman <sup>1</sup> , Briana Hauff-Salas <sup>2,\*</sup> , Joshua A. Haslun <sup>3</sup>, James M. Cervino <sup>4</sup> and Kevin B. Strychar <sup>5</sup>

<sup>1</sup> National Centers for Coastal Ocean Science, National Oceanic and Atmospheric Administration, Beaufort, NC 28516, USA; tyler.harman@noaa.gov

<sup>2</sup> Department of Mathematics and Science, Our Lady of the Lake University, San Antonio, TX 78207, USA

<sup>3</sup> Lux Research, Inc., Emerging Ecosystems in Agrifood and Health, 100 Franklin Street, Boston, MA 02110, USA; Joshua.Haslun@luxresearchinc.com

<sup>4</sup> Department of Marine Chemistry & Geochemistry, Woods Hole Oceanographic Institute, Woods Hole, MA 02543, USA; jamescervino@gmail.com

<sup>5</sup> Annis Water Resources Institute, Grand Valley State University, Muskegon, MI 49441, USA; strychak@gvsu.edu

\* Correspondence: bhsalas@ollusa.edu



**Citation:** Harman, T.E.; Hauff-Salas, B.; Haslun, J.A.; Cervino, J.M.; Strychar, K.B. Decreased Photosynthetic Efficiency in Response to Site Translocation and Elevated Temperature Is Mitigated with LPS Exposure in *Porites astreoides* Symbionts. *Water* **2022**, *14*, 366. <https://doi.org/10.3390/w14030366>

Academic Editor: José Luis Sánchez-Lizaso

Received: 24 November 2021

Accepted: 23 January 2022

Published: 26 January 2022

**Publisher's Note:** MDPI stays neutral with regard to jurisdictional claims in published maps and institutional affiliations.



**Copyright:** © 2022 by the authors. Licensee MDPI, Basel, Switzerland. This article is an open access article distributed under the terms and conditions of the Creative Commons Attribution (CC BY) license (<https://creativecommons.org/licenses/by/4.0/>).

**Abstract:** Coral reefs have been detrimentally impacted causing health issues due to elevated ocean temperatures as a result of increased greenhouse gases. Extreme temperatures have also exacerbated coral diseases in tropical reef environments. Numerous studies have outlined the impacts of thermal stress and disease on coral organisms, as well as understanding the influence of site-based characteristics on coral physiology. However, few have discussed the interaction of all three. Laboratory out-planting restoration projects have been of importance throughout impacted areas such as the Caribbean and southern Florida in order to increase coral cover in these areas. This study analyzes photosynthetic efficiency of *Porites astreoides* from the lower Florida Keys after a two-year reciprocal transplant study at inshore (Birthday reef) and offshore (Acer24 reef) sites to understand acclimation capacity of this species. Laboratory experiments subjected these colonies to one of three treatments: control conditions, increases in temperature, and increases in temperature plus exposure to an immune stimulant (lipopolysaccharide (LPS)) to determine their influence on photosynthetic efficiency and how stress events impact these measurements. In addition, this study is a continuation of previous studies from this group. Here, we aim to understand if these results are static or if an acclimation capacity could be found. Overall, we observed site-specific influences from the Acer24 reef site, which had significant decreases in photosynthetic efficiencies in 32 °C treatments compared to Birthday reef colonies. We suggest that high irradiance and lack of an annual recovery period from the Acer24 site exposes these colonies to significant photoinhibition. In addition, we observed significant increases in photosynthetic efficiencies from LPS exposure. We suggest host-derived antioxidants can mitigate the negative impacts of increased thermal stress. Further research is required to understand the full complexity of host immunity and symbiont photosynthetic interactions.

**Keywords:** pulse-amplitude modulated fluorometry; innate immunity; Symbiodiniaceae; Florida Keys; lipopolysaccharide; coral disease

## 1. Introduction

Increases in atmospheric greenhouse gases from anthropogenic activities have contributed to climate change by trapping more solar radiation from the sun and warming the planet [1,2]. Ocean temperatures have risen concurrently with atmospheric temperatures, negatively impacting marine organisms [3]. One of the most thermally sensitive marine ecosystems are coral reefs. Coral reefs exist and thrive within a narrow range of

light, temperature, salinity, and turbidity [4]. This is due to the symbiotic relationship that coral organisms have with algae in the family Symbiodiniaceae. Symbiodiniaceae live inside the tissues of corals and provide sustenance to their coral hosts via translocation of photosynthetic byproducts [5,6]. Corals rely heavily on this mutualistic relationship as algae provide up to 90% of the coral hosts daily metabolic needs [6,7]. As temperatures have risen over the past several decades so have incidences of coral bleaching, or rather, expulsion of symbiotic algae from the coral host. In addition, light is also a significant impact on coral bleaching and reductions in photosynthetic efficiencies and symbiont pigmentation [8]. Oxidative stress is a significant effect on coral bleaching, where stress events (i.e., temperature and light) impact repair mechanisms and cause cascading events such as reductions in photosynthetic efficiencies, and eventual expulsion of symbionts by means of apoptosis, necrosis, and exocytosis [8]. Depending on the duration and severity of the event, bleaching can significantly contribute to coral mortality [9]. Bleaching has caused many coral reefs around the world to lose significant amounts of coral cover such as in southern Florida (USA) and the Great Barrier Reef (Australia) [10,11].

Although thermal stress continues to be a substantial threat to corals worldwide, disease is another prominent challenge in coral survivorship. Coral diseases can consist of a consortium of various pathogens that collectively promote diseases such as yellow-band disease (YBD), white-band disease (WBD), and stony coral tissue loss disease (SCTLD) [12–14] and may target specific regions of a coral host. For example, YBD is found to specifically affect symbiotic algae via cell dysfunction and reduced division [12,15,16], and WBD and SCTLD affect the coral host directly [13,14]. When pathogens encounter a coral host, microbial-associated molecular patterns (MAMPs, i.e., lipopolysaccharide) on pathogenic bacteria bind to pattern recognition receptors (PRRs; toll-like receptors, peptidoglycan recognition proteins, C-type lectins, etc.) associated with coral host cells [17,18]. Binding of MAMPs and PRRs have been shown to initiate immunological pathways in coral organisms [19,20]. As such, multiple immune pathways have evolved within cnidarians to include the Toll receptor pathway, complement pathway, and the melanin synthesis pathway [17,21–24]. Each represents a particular protective response to mitigate pathogenic infection, including opsonization and/or antioxidation [17,20]. For example, the melanin synthesis pathway associated with coral host antioxidants is generated to mitigate pathogenic infection [17,20].

Several studies have identified the impact of disease on Symbiodiniaceae in regard to host-associated immune responses [12,15,16]. It has been postulated that the consortium of *Vibrio* causing YBD directly impacts organelles and photosynthetic components within Symbiodiniaceae, resulting in reduced pigmentation and lower quantum yield [16]. Differences in gene expression regarding transporter activities have been reported [25], hypothesizing a dysbiosis response of the coral host with Symbiodiniaceae in regard to disease exposure, but a previous study [25] stressed that further research is needed. Research of disease impacts to Symbiodiniaceae show the plausibility of photo-physiology degradation and other indirect effects. Indications of the impacts of disease on Symbiodiniaceae photo-physiology are outlined previously, where the reduction of a coral host's micro-shading environment by disease directly impacting host tissue may exacerbate bleaching effects [26]. On the other hand, host-derived antioxidants also play a role in mitigating photosynthetically generated reactive oxygen species (ROS), potentially benefitting photosynthetic health [27].

Physiological acclimation to stressful scenarios by means of altered gene expression is another avenue for resilience in coral organisms to combat thermal stress events through apoptosis and immune regulation [28], or upregulation of heat shock proteins and transcription factors [29,30]. Species-specific responses (e.g., protein and lipid concentrations, gene expression, etc.) and site-specific factors (e.g., duration and magnitude of thermal stress) need to be taken into consideration to determine accurate resilience to thermal anomalies [31].

To better understand the relationship between thermal stress, coral disease, and short-term physiological acclimation on photosynthetic efficiencies in corals, we exposed

*Porites astreoides*, a common tropical coral species found in the Florida Keys, to a two-year reciprocal transplant experiment. A subset of corals was moved from a low-bleaching reef to a high-bleaching reef, and vice versa, for two years, while others remained in their native population. After two years in the field, *P. astreoides* fragments were subjected to laboratory-controlled elevated temperature conditions with and without the presence of a coral disease agent (Lipopolysaccharide from *Serratia marcescens*). A typical example of a MAMP, lipopolysaccharide (LPS) elicits a strong immune response through recognition via host PRRs, as stated previously [32]. The use of LPS here allowed us to dictate a straightforward response to disease from coral symbionts rather than the complex responses of live pathogens. Both effective quantum yield ( $Fv'/Fm'$ ) and maximum quantum yield ( $Fv/Fm$ ) were used as proxies to determine photosynthetic efficiency in *P. astreoides*.

Overall, the goal of this study is to determine if *Porites astreoides* has the capacity to acclimate to new conditions within a dictated time frame. Ideally, this study's laboratory exposure helps demonstrate the success of the fragments ability to acclimate to the new environment (genotype by environment interactions) and understand its overall success and plasticity to new environmental factors. Will these fragments fair better or worse when exposed to (a) stress event(s)? Transplant restoration projects are of importance to combat significant declines of coral cover in Caribbean and southern Florida reefs [33–35]. In addition, disease outbreaks in these areas are another significant obstacle that restoration projects must account for. This study is reciprocal to a previous study [32] where similar conditions were demonstrated but focused primarily on specific gene expression. Laboratory conditions from the previous study dictated no differences between reef fragments regarding short-term stress events. In addition to our overall goal, we also seek to understand if the results of this study have static responses, such as in [32], or will these fragments have the capacity to acclimate from short-term translocation.

## 2. Materials and Methods

### 2.1. Reciprocal Transplant and Sample Collection

Fragments of *Porites astreoides* reciprocally transplanted from an inshore and offshore site in the lower Florida Keys were analyzed for changes in maximum and effective quantum yield after exposure to elevated temperatures and lipopolysaccharide (LPS) of *Serratia marcescens* in a lab experiment. A more in-depth discussion of study sites, initial coral collection, reciprocal transplant, and laboratory experimental design can be found in our previous studies [32,36,37] and explained in more depth below.

Briefly, ten whole colonies ( $16 \times 16$  cm) of *P. astreoides* were collected from Birthday Reef (inshore: 24.57917° N–81.49693° W) and an additional ten whole colonies ( $16 \times 16$  cm) of *P. astreoides* were collected from Acer24 Reef (offshore: 24.55268° N–81.43741° W) (Permit #FKNMS-2011-107, Florida Keys National Marine Sanctuary) (Figure 1). Both reef sites are patch reefs in the lower Florida Keys, separated by Hawk Channel. Biotic and abiotic conditions are similar at each reef (i.e., species composition, depth) except for notably distinct temperature and turbidity regimes. Compared to Birthday Reef, Acer24 reef had significantly lower turbidity and Chl-a regimes, higher light, lower variation in winter temperatures (20–25 °C vs. 18–29 °C) and a higher incidence of coral bleaching [37]. As discussed in Haslun et al. [37], a principal coordinate analysis (PCA) was conducted using subsets of a Water Quality Monitoring Project dataset that included biotic and abiotic measurements from Acer24 and Birthday Reefs, as well as neighboring inshore and offshore reefs. The goal of this analysis was to identify factors associated with increased coral stress during winter and summer periods and to identify any potential differences between inshore and offshore reefs. Analysis found that PC2, which included Chl-a, explained 19.2% of variation between sites, and PC3, which included temperature and turbidity explained 13.1% of variation between sites. Additionally, further investigation by Haslun et al. [37] found increased levels of bleaching of *P. astreoides* fragments at Acer24 reef as measured by coral brightness and effective quantum yield ( $Fv'/Fm'$ ).



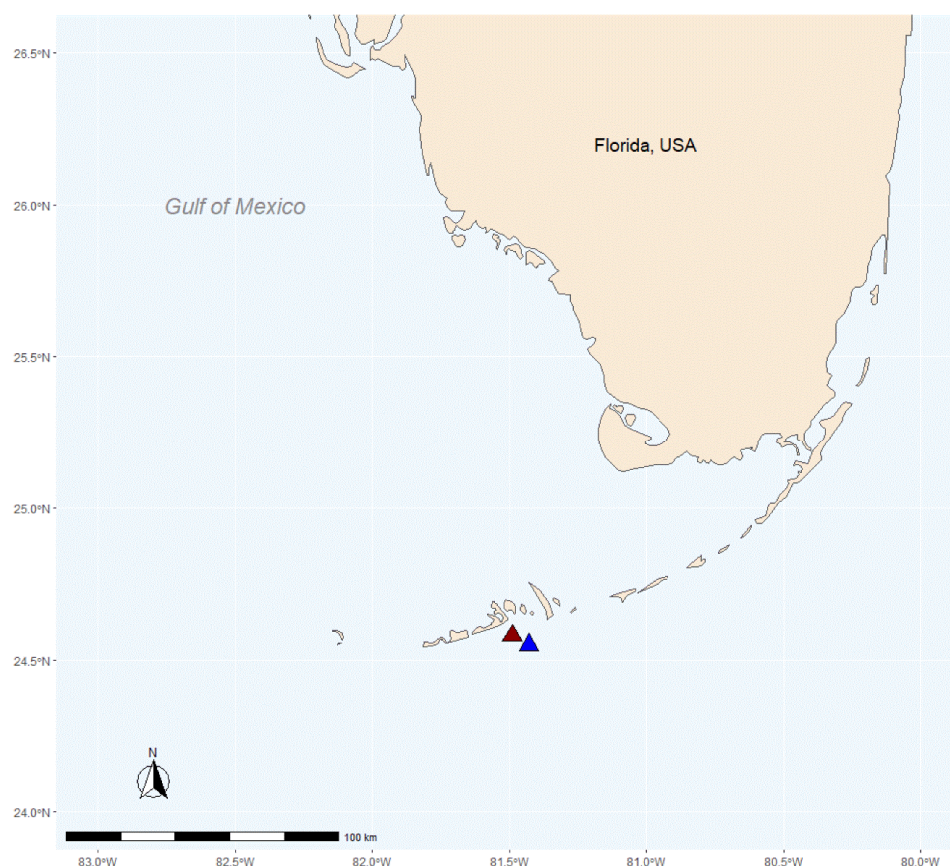


**Figure 1.** Site map of the inshore Birthday reef (red triangle: 24.57917° N–81.49692° W) and the offshore Acer24 reef (blue triangle: 24.55268° N–81.43741° W) locations within the lower Florida Keys.

After collection, the 20 fragments of *P. astreoides* were transported to Mote Marine Tropical Laboratory (MMTL) where they were sectioned into equal halves ( $n = 40$ ). Halves were then reciprocally transplanted back on to the reefs, with one half returning to its reef of origin and the other half transplanted to the other reef. For example, half a fragment from an Acer24 Reef sample was returned to Acer24 Reef, while the other half was transplanted to Birthday Reef [32]. Fragments remained at the reciprocal reef sites for two years (August 2011–August 2013).

Upon completion of the field experiment, all fragments of *P. astreoides* ( $n = 40$ ) were collected and returned to MMTL where they were sectioned into nine, approximately  $2 \times 2$  cm fragments each, for a total of  $n = 360$  samples. Coming from the same parent colony, these nine fragments are considered pseudo-replicates. Fragments were allowed to recover for at least 72 h in a shaded flow through water table (680-L fiberglass trough) prior to the laboratory experiment (for greater detail see in [32]).

## 2.2. Temperature and LPS Experiment with Pulse Amplitude Modulation (PAM) Measurements

Briefly, the laboratory experiment consisted of a one-way design with three experimental levels: 28 °C (control, ambient temperature of water tables), 32 °C (temperature known to cause bleaching [38,39]), and 32 °C + LPS (bleaching temperatures combined with simulating a bacterial infection). Purified LPS from *S. marcescens* was used in lieu of whole bacteria to minimize cross-contamination into the surrounding environment as MMTL's flow through tank systems connect directly to the adjacent channel and the Florida Keys waterways. Additional precautions were taken to not add purified LPS to flow through sections of the experimental design. Each treatment was replicated in two tanks (details below) for six independent units of analysis.

As outlined previously [32], experimental set up included six 38 L fish tanks set within a water table; two 38 L tanks for each experimental level. Five custom-made acrylic boxes ( $2.5 \times 7.5 \times 7.5$  cm) were set within each 38 L fish tank. Each custom acrylic box had three independent subdivisions, and each housing a single coral fragment ( $n = 90$ ). Fish tanks were filled with water from the water table, while acrylic boxes were filled with artificial sterile seawater (ASSW) (Figure 2). The experiment was repeated eight times as detailed below and included a final sample number of  $n = 720$  samples.

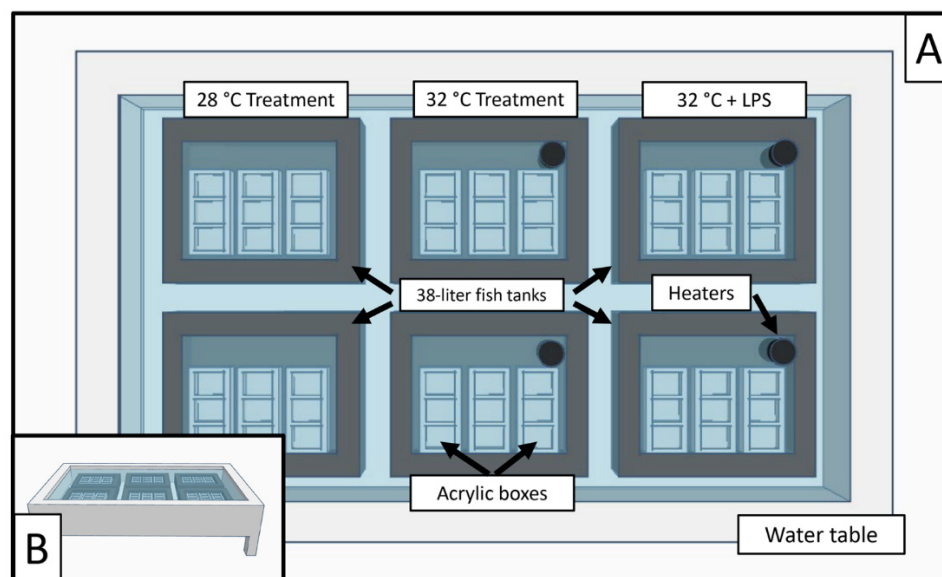


**Figure 2.** (A) A 3D model overview of the experimental aquarium system. Six individual 38 L tanks were placed within a 680 L water table. Custom acrylic boxes were placed within each 38 L tank, separated into three sections, and filled with ASSW. Heaters were placed in the 38 L tanks if elevated temperatures were a part of the treatment. (B) A zoomed-out 3D model of the 680 L water table.

Coral fragments were removed from their holding tanks (680 L fiberglass trough), rinsed with ASSW, and placed into acrylic box subsections at experimental temperatures. Heaters were placed external to the acrylic boxes to maintain elevated temperatures in the 32 °C and 32 °C + LPS treatments ( $32 \text{ °C} \pm 0.5$ ) and monitored with HOBO tags (Onset Computer Corporations, Bourne MA, USA). For the 32 °C + LPS treatments, LPS from *S. marcescens* (1 mL, 5 µg/mL) [32,40] was added to ASSW when the coral fragment was transferred to the acrylic boxes. For consistency, 1mL of ASSW was added to the 28 °C and 32 °C treatments. Corals were exposed to treatments for a total of eight hours. Every hour, subdivisions were aerated via air infusion using disposable pipettes, taking care not to disturb the coral.

Measurements of maximum ( $F_v/F_m$ ) and effective ( $F_v'/F_m'$ ) quantum yield were taken using a diving PAM fluorometer (Walz, Germany).  $F_v'/F_m'$  ratios dictate the amount of light that is absorbed by chlorophyll in photosystem II (PSII). Higher proportions of light absorbed correspond to higher efficiencies while lower proportions correspond to lowered overall photosynthesis [41]. Observing changes to photosynthetic efficiency allows us to determine how stress impacts the photosynthetic capacity of the holobiont.  $F_v/F_m$  ratios are equally as important to detect the overall maximum efficiency, or overall photosynthetic performance of PSII reaction centers, as decreases in  $F_v/F_m$  are an indicator of increased stress experienced by algae [41]. Here, maximum quantum yield of photochemical energy conversion is seen as a function of Symbiodiniaceae sp. photosynthetic efficiency. One day prior to experimentation, yield measurements were taken to compare to experimental controls. During experimentation, measurements of effective quantum yield were taken at 1200 h, and maximum quantum yield at 1700 h.

### 2.3. Data Analysis

All data were organized within Microsoft Excel, and all manipulation and statistical analyses were completed within RStudio [42] under R Version 4.0.0 [43]. Exploratory analysis of the data revealed it to be nonparametric, using Shapiro–Wilk tests. Statistical analyses were done using Kruskal–Wallis tests on *P. astreoides* fragments subjected to 28 °C temperature treatments before the experiments and during the experiments to detect changes in effective/maximum quantum yield ratios from tank effect. All  $Fv/Fm$  and  $Fv'/Fm'$  data were run through generalized mixed linear models (GMLM) with an inverse Gaussian distribution correction, selecting treatment and translocation as fixed effects and fragment number categorized as a random effect (Figures A1 and A2; Tables A1 and A2). Furthermore, a “post hoc” least square means analysis (package *lsmeans*) [44] was done to detect significant differences between relevant comparisons.

### 3. Results

Differences in  $Fv'/Fm'$  (Figure 3A) and  $Fv/Fm$  (Figure 3B) from 28 °C control temperature treatments taken before (i.e., in holding tanks the day prior to experimentation), and then during experimentation, show significantly lower ratios in both  $Fv'/Fm'$  and  $Fv/Fm$  measurements during the experiments within the “Acer24 to Acer24” (hereafter AA) translocation site ( $p \leq 0.05$ ), while all other sites displayed no statistical differences.

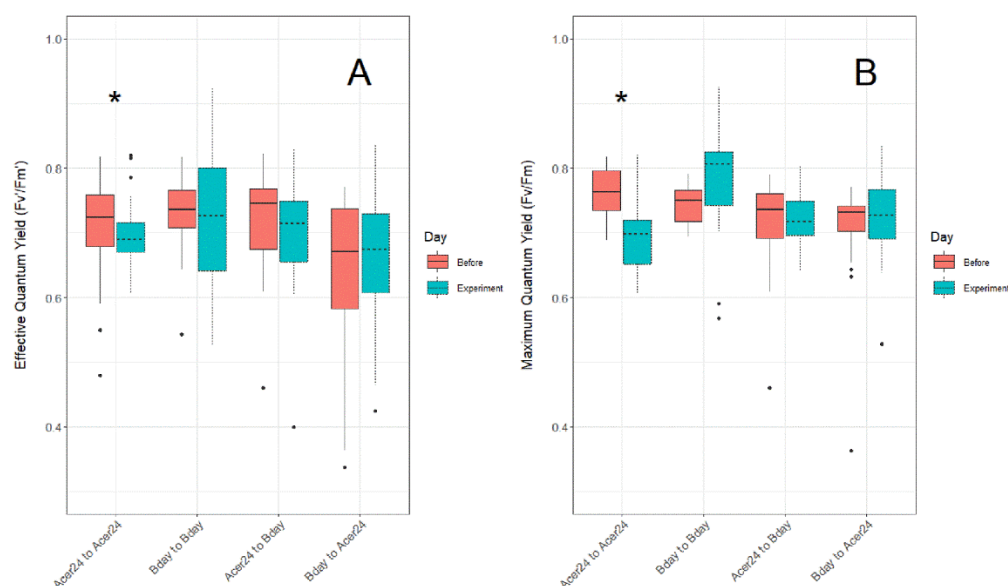


**Figure 3.** Difference in (A) effective quantum yield ratios ( $Fv'/Fm'$ ) and (B) maximum quantum yield ratios ( $Fv/Fm$ ) in *Porites astreoides* treated in 28 °C temperature treatments between before and during experiments to detect issues regarding experimental tank effect. Asterisk above clustered boxplots indicate significant difference ( $p \leq 0.05$ ) in effective quantum yield and maximum quantum yield values.

#### 3.1. Quantum Yield ( $Fv'/Fm'$ )

Pairwise comparison results from Acer24 translocated colonies found that  $Fv'/Fm'$  from AA samples was significantly lower in 32 °C treatments when compared to 28 °C ( $p \leq 0.05$ ; Figure 4, Table 1), but no significant difference was found when comparing the remaining treatments. In addition,  $Fv'/Fm'$  from “Birthday to Acer24” (hereafter BA) was significantly lower in 32 °C treatments when compared to 28 °C treatments ( $p \leq 0.05$ ; Figure 4, Table 1), and significantly higher in 32 °C + LPS treatment when compared to both 28 °C and 32 °C treatments ( $p \leq 0.05$ ; Figure 4, Table 1).  $Fv'/Fm'$  results from Birthday translocated sites found no significant difference between temperature and LPS treatments for “Acer24 to Birthday” (hereafter AB) samples or “Birthday to Birthday” (hereafter BB) samples.

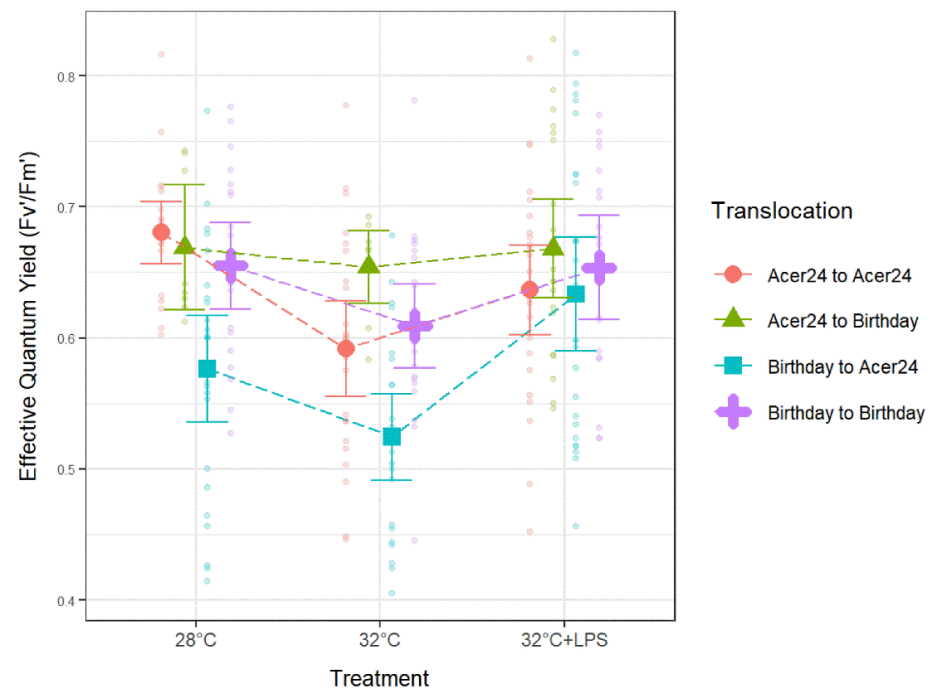


**Figure 4.** Effective quantum yield in *Porites astreoides* based on treatment separated by translocation site. The triangle shapes represent mean effective quantum yield values and error bars represent  $\pm 95\%$  confidence intervals. Transparent circles represent individual effective quantum yield measurements to visually represent the spread of the data.

**Table 1.** Least square means pairwise comparison results of effective quantum yield ( $Fv'/Fm'$ ) between translocated sites and between laboratory experimental conditions. Bolded and highlighted  $p$ -values indicate significant differences of effective quantum yield results.

Contrast	Estimate	SE	df	z Ratio	p Value
Acer to Acer.28 °C–Acer to Acer.32 °C	−0.69441	0.203	Inf	−3.429	<b>0.0006</b>
Acer to Acer.28 °C–(Acer to Acer.32 °C + LPS)	−0.30682	0.189	Inf	−1.622	0.1048
Acer to Acer.28 °C–Acer to Birthday.28 °C	−0.07381	0.256	Inf	−0.288	0.7734
Acer to Acer.28 °C–Birthday to Acer.28 °C	−0.85011	0.207	Inf	−4.104	<b>0.0001</b>
Acer to Acer.28 °C–Birthday to Birthday.28 °C	−0.16985	0.193	Inf	−0.878	0.3799
Acer to Acer.32 °C–(Acer to Acer.32 °C + LPS)	0.3876	0.201	Inf	1.924	0.0544
Acer to Acer.32 °C–Acer to Birthday.32 °C	0.51777	0.261	Inf	1.983	<b>0.0474</b>
Acer to Acer.32 °C–Birthday to Acer.32 °C	−0.78198	0.239	Inf	−3.267	<b>0.0011</b>
Acer to Acer.32 °C–Birthday to Birthday.32 °C	0.15949	0.217	Inf	0.736	0.4616
(Acer to Acer.32 °C + LPS)–(Acer to Birthday.32 °C + LPS)	0.22715	0.189	Inf	1.199	0.2304
(Acer to Acer.32 °C + LPS)–(Birthday to Acer.32 °C + LPS)	−0.0251	0.187	Inf	−0.134	0.8932
(Acer to Acer.32 °C + LPS)–(Birthday to Birthday.32 °C + LPS)	0.12754	0.198	Inf	0.645	0.5192
Acer to Birthday.28 °C–Acer to Birthday.32 °C	−0.10283	0.305	Inf	−0.337	0.7358
Acer to Birthday.28 °C–Acer to Birthday.32 °C + LPS)	−0.00586	0.257	Inf	−0.023	0.9818
Acer to Birthday.28 °C–Birthday to Acer.28 °C	−0.7763	0.269	Inf	−2.885	<b>0.0039</b>
Acer to Birthday.28 °C–Birthday to Birthday.28 °C	−0.09604	0.259	Inf	−0.371	0.7104
Acer to Birthday.32 °C–(Acer to Birthday.32 °C + LPS)	0.09697	0.252	Inf	0.385	0.7003
Acer to Birthday.32 °C–Birthday to Acer.32 °C	−1.29975	0.282	Inf	−4.606	<b>0.0001</b>
Acer to Birthday.32 °C–Birthday to Birthday.32 °C	−0.35828	0.263	Inf	−1.361	0.1735
(Acer to Birthday.32 °C + LPS)–(Birthday to Acer.32 °C + LPS)	−0.25225	0.188	Inf	−1.34	0.1804
(Acer to Birthday.32 °C + LPS)–(Birthday to Birthday.32 °C + LPS)	−0.09961	0.199	Inf	−0.5	0.617
Birthday to Acer.28 °C–Birthday to Acer.32 °C	−0.62628	0.243	Inf	−2.574	<b>0.01</b>
Birthday to Acer.28 °C–(Birthday to Acer.32 °C + LPS)	0.51819	0.205	Inf	2.527	<b>0.0115</b>
Birthday to Acer.28 °C–Birthday to Birthday.28 °C	0.68026	0.21	Inf	3.238	<b>0.0012</b>



Table 1. Cont.

Contrast	Estimate	SE	df	z Ratio	p Value
Birthday to Acer.32 °C–(Birthday to Acer.32 °C + LPS)	1.14448	0.227	Inf	5.037	0.0001
Birthday to Acer.32 °C–Birthday to Birthday.32 °C	0.94147	0.242	Inf	3.896	0.0001
(Birthday to Acer.32 °C + LPS)–(Birthday to Birthday.32 °C + LPS)	0.15264	0.197	Inf	0.776	0.438
Birthday to Birthday.28 °C–Birthday to Birthday.32 °C	−0.36508	0.208	Inf	−1.754	0.0795
Birthday to Birthday.28 °C–(Birthday to Birthday.32 °C + LPS)	−0.00943	0.202	Inf	−0.047	0.9628
Birthday to Birthday.32 °C–(Birthday to Birthday.32 °C + LPS)	0.35565	0.213	Inf	1.667	0.0955

Regarding comparisons between translocation sites,  $Fv'/Fm'$  ratios trended with decreases in response to 32 °C treatments when compared to 28 °C treatments and a subsequent increase with 32 °C + LPS treatments to levels similar or higher than 28 °C treatments (Figure 4; Table 1). No significant differences were found between translocation sites within the 32 °C + LPS treatment. Within 28 °C treatments, BA samples had significantly lower  $Fv'/Fm'$  when compared to all other translocation sites ( $p \leq 0.05$ ; Figure 4; Table 1). Within 32 °C treatments, AA samples had significantly lower  $Fv'/Fm'$  when compared to AB samples ( $p \leq 0.05$ ; Figure 4; Table 1), BA samples also had significantly lower  $Fv'/Fm'$  when compared to all other translocations at the 32 °C treatments ( $p \leq 0.05$ ; Figure 4, Table 1).

### 3.2. Maximum Quantum Yield ( $Fv/Fm$ )

Within AA samples,  $Fv/Fm$  was significantly lower at 32 °C when compared to 32 °C + LPS ( $p \leq 0.05$ ; Figure 5, Table 2), while  $Fv/Fm$  of BA samples was significantly lower at 32 °C when compared to both controls (28 °C) and 32 °C + LPS ( $p \leq 0.05$ ; Figure 5, Table 2).  $Fv/Fm$  of AB samples was significantly lower at 32 °C + LPS when compared to 28 °C controls ( $p \leq 0.05$ ; Figure 5, Table 2) and BB samples were significantly lower at 32 °C when compared to controls ( $p \leq 0.05$ ; Figure 5, Table 2).

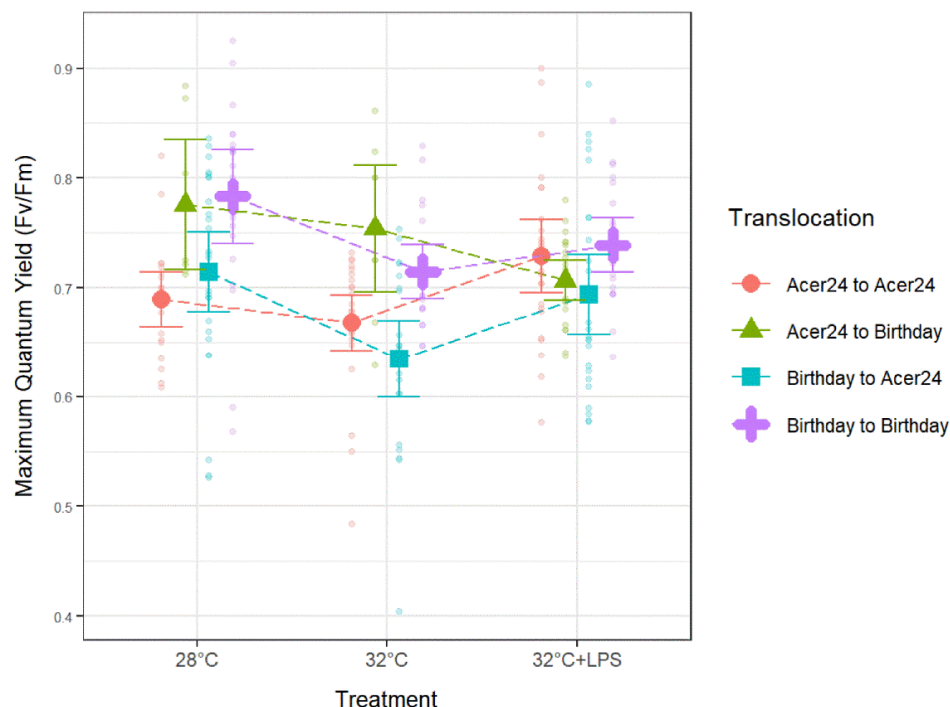


**Figure 5.** Maximum quantum yield in *Porites astreoides* based on treatment separated by translocation site. The triangle shapes represent mean maximum quantum yield values and error bars represent  $\pm 95\%$  confidence intervals. Transparent circles represent individual maximum quantum yield measurements to visually represent the spread of the data.



**Table 2.** Least square means pairwise comparison results of maximum quantum yield ( $Fv/Fm$ ) between translocated sites and between laboratory experimental conditions. Bolded and highlighted  $p$ -values indicate significant differences of maximum quantum yield results.

Contrast	Estimate	SE	df	z Ratio	p Value
Acer to Acer.28 °C–Acer to Acer.32 °C	−0.13682	0.133	Inf	−1.032	0.3019
Acer to Acer.28 °C–(Acer to Acer.32 °C + LPS)	0.22421	0.125	Inf	1.794	0.0728
Acer to Acer.28 °C–Acer to Birthday.28 °C	0.44417	0.159	Inf	2.796	<b>0.0052</b>
Acer to Acer.28 °C–Birthday to Acer.28 °C	0.14601	0.125	Inf	1.173	0.2409
Acer to Acer.28 °C–Birthday to Birthday.28 °C	0.47585	0.124	Inf	3.833	<b>0.0001</b>
Acer to Acer.32 °C–(Acer to Acer.32 °C + LPS)	0.36103	0.122	Inf	2.963	<b>0.0031</b>
Acer to Acer.32 °C–Acer to Birthday.32 °C	0.48374	0.155	Inf	3.126	<b>0.0018</b>
Acer to Acer.32 °C–Birthday to Acer.32 °C	−0.24104	0.136	Inf	−1.767	0.0772
Acer to Acer.32 °C–Birthday to Birthday.32 °C	0.28525	0.129	Inf	2.213	<b>0.0269</b>
(Acer to Acer.32 °C + LPS)–(Acer to Birthday.32 °C + LPS)	−0.12109	0.121	Inf	−1.004	0.3155
(Acer to Acer.32 °C + LPS)–(Birthday to Acer.32 °C + LPS)	−0.19596	0.116	Inf	−1.695	0.0901
(Acer to Acer.32 °C + LPS)–(Birthday to Birthday.32 °C + LPS)	0.05058	0.116	Inf	0.435	0.6637
Acer to Birthday.28 °C–Acer to Birthday.32 °C	−0.09725	0.178	Inf	−0.547	0.5844
Acer to Birthday.28 °C–(Acer to Birthday.32 °C + LPS)	−0.34105	0.155	Inf	−2.194	<b>0.0282</b>
Acer to Birthday.28 °C–Birthday to Acer.28 °C	−0.29816	0.15	Inf	−1.992	<b>0.0463</b>
Acer to Birthday.28 °C–Birthday to Birthday.28 °C	0.03167	0.149	Inf	0.212	0.8321
Acer to Birthday.32 °C–(Acer to Birthday.32 °C + LPS)	−0.2438	0.154	Inf	−1.585	0.1129
Acer to Birthday.32 °C–Birthday to Acer.32 °C	−0.72478	0.161	Inf	−4.515	<b>0.0001</b>
Acer to Birthday.32 °C–Birthday to Birthday.32 °C	−0.19849	0.154	Inf	−1.287	0.198
(Acer to Birthday.32 °C + LPS)–(Birthday to Acer.32 °C + LPS)	−0.07488	0.123	Inf	−0.611	0.5411
(Acer to Birthday.32 °C + LPS)–(Birthday to Birthday.32 °C + LPS)	0.17167	0.123	Inf	1.393	0.1635
Birthday to Acer.28 °C–Birthday to Acer.32 °C	−0.52387	0.129	Inf	−4.073	<b>0.0001</b>
Birthday to Acer.28 °C–(Birthday to Acer.32 °C + LPS)	−0.11776	0.115	Inf	−1.023	0.3062
Birthday to Acer.28 °C–Birthday to Birthday.28 °C	0.32984	0.112	Inf	2.941	<b>0.0033</b>
Birthday to Acer.32 °C–(Birthday to Acer.32 °C + LPS)	0.40611	0.131	Inf	3.103	<b>0.0019</b>
Birthday to Acer.32 °C–Birthday to Birthday.32 °C	0.52629	0.136	Inf	3.877	<b>0.0001</b>
(Birthday to Acer.32 °C + LPS)–(Birthday to Birthday.32 °C + LPS)	0.24654	0.118	Inf	2.084	<b>0.0371</b>
Birthday to Birthday.28 °C–Birthday to Birthday.32 °C	−0.32741	0.12	Inf	−2.723	<b>0.0065</b>
Birthday to Birthday.28 °C–(Birthday to Birthday.32 °C + LPS)	−0.20105	0.115	Inf	−1.742	0.0815
Birthday to Birthday.32 °C–(Birthday to Birthday.32 °C + LPS)	0.12636	0.124	Inf	1.022	0.3069

Similar to  $Fv'/Fm'$ , between translocation sites  $Fv/Fm$  ratios trended with decreases in response to 32 °C treatments when compared to 28 °C treatments and a slight increase with 32 °C + LPS treatments, but not to levels higher than 28 °C treatments (Figure 5; Table 2). This trend is apparent for all translocation sites, except AB whose  $Fv/Fm$  ratios decreased at 32 °C + LPS when compared to both controls (28 °C) and 32 °C. Within 28 °C treatments, AA  $Fv/Fm$  was significantly lower than AB and BB samples, and BA  $Fv/Fm$  was significantly lower than AB and BB samples ( $p \leq 0.05$ ; Figure 5; Table 2). Within 32 °C treatments, AA  $Fv/Fm$  was significantly lower than AB and BB samples, and BA  $Fv/Fm$  was significantly lower than AB and BB samples ( $p \leq 0.05$ ; Figure 5; Table 2). Finally, within the 32 °C + LPS treatments, BA  $Fv/Fm$  was significantly lower than BB samples ( $p \leq 0.05$ ; Figure 5; Table 2).

#### 4. Discussion

PAM fluorometry is a useful tool to detect differences in photosynthetic efficiency of symbiotic coral algae by means of effective ( $Fv'/Fm'$ ) and maximum ( $Fv/Fm$ ) quantum yield ratios. Here, we used PAM fluorometry to examine the potential for acclimation of two populations of *Porites astreoides* to novel environmental conditions. Our results demonstrate acclimation as indicated by a transplant site-specific effect for both effective and maximum quantum yield ratios involving in situ high-irradiance stress from Acer24 site origins. We also demonstrate that the photosynthetic efficiency was not impaired by LPS (e.g., simulation of disease), potentially influenced from host-derived ROS suppressants. While it is out of the scope of this paper, this information could be useful for coral repopulation efforts in southern Florida [45] as our results indicate the importance of thermal history to the resiliency of photosynthetic efficiency changes in response to thermal stress. The changes in effective ( $Fv'/Fm'$ ) and maximum ( $Fv/Fm$ ) quantum yield ratios observed

in our study improve the understanding of *P. asteroides*, a critical reef building species in the Florida Keys, and susceptibility to the synergistic effects of elevated temperatures and disease [19,46].

Prior to any experiment,  $Fv'/Fm'$  and  $Fv/Fm$  were measured in each of the holding tanks. These measurements were compared to  $Fv'/Fm'$  and  $Fv/Fm$  values of control fragments during the experiment to assess potential tank effects. Indications of tank effects were found within AA fragments as  $Fv'/Fm'$  and  $Fv/Fm$  values were significantly lower in 28 °C experimental fragments ( $p \leq 0.05$ , Figure 3) when compared to holding tank measurements. As AA fragments were the first set of experiments run, it is possible that reduced acclimation time within the holding tanks compared to other translocation site fragments of *P. astreoides* caused these differences in quantum yield. AA fragments were given three days of acclimation in laboratory aquarium systems compared to the remaining fragments which had between four and ten days. If the tank effect present was due to a reduced acclimation time and not a “true” difference, meaning that stress was involved and had not been mitigated, we can assume that our data for AA would be significantly higher than the current data we provide. We surmise that  $Fv'/Fm'$  and  $Fv/Fm$  data from AA translocation sites could be similar to, or higher than, AB and BB translocation sites.

Between our experimental treatments, fragments replaced at Acer24 reef (i.e., AA and BA) and exposed to 32 °C showed significantly lower  $Fv'/Fm'$  and  $Fv/Fm$  ratios compared to translocation sites with a final destination of Birthday reef exposed to the same conditions. Differences of  $Fv'/Fm'$  and  $Fv/Fm$  ratios suggest site-specific characteristics of Acer24 reef that stimulated a reduction of photosynthetic capacity. Our accompanying study [37] suggested the importance of seasonal recovery from increased irradiance in offshore (Acer24) sites compared to inshore (Birthday) sites. Higher irradiance is associated with bleaching and is observed at Acer24 reef compared to the Birthday reef site, which is considerably more turbid, thus reducing irradiance-related stress [37]. In situ temperatures on Birthday and Acer24 sites were similar to the same degree, but irradiance was the only abiotic difference measured that may have drove the Acer24 site coral to reduced photosynthetic efficiencies. In addition, irradiance stress has been found to significantly impact photosynthetic electron transport resulting in decreased photosynthetic efficiencies [47]. This may explain the susceptibility in translocated fragments from the Acer24 reef site. Acer24 fragments may experience a reduced, or completely lack, (a) recovery period during the winter months thus leaving them more probable to reduced photosynthetic efficiency when experiencing thermal or irradiance stress. Reductions in recovery over a winter season can cause significant photoinhibition in offshore sites compared to inshore sites which can result in lower quantum efficiencies [48,49]. In addition, high irradiance acclimated corals show lower pigment concentrations and shifts in chloroplast organization [50], and subsequently reduced absorption capabilities result in lower photosynthetic efficiencies [51,52]. Finally, translocation to environmentally stressful sites from native sites (such as BA) can induce reduced physiological plasticity (i.e., reduced effective and maximum quantum yields) compared to natives in environmentally stressful locations (i.e., AA samples) [29,31]. These findings together suggest how site-specific characteristics play a significant role in the physiological responses of thermal stress.

Decreases in  $Fv'/Fm'$  exhibited by fragments located at the Acer24 site may also be the result of decreases in symbiotic algae populations [53] due to more frequent bleaching conditions experienced at Acer24 Reef [36]. Bleaching-related stress increases the concentration of reactive oxygen species (ROS) such as singlet oxygen and hydrogen peroxide within photosynthetic organisms and degrades PSII, leading to bleaching [54–57]. Increased bleaching was documented at Acer24 reef during the transplant experiment when compared to Birthday Reef [36]. Therefore, reductions in algae concentrations may be likely along with photoinhibition as stated in the previous paragraph, which, when combined, exacerbate the decrease in quantum efficiencies observed here. Additionally, distinct changes in Symbiodiniaceae populations within our *P. astreoides* fragments over the two-year acclimation period were reported previously [36]. Changes in *Symbiodinium linucheae* (Trench & Thinh)

(formerly clade A4) ITS2-subclades A4.1, A4.2, and A4.3 frequencies were measured before and after translocation experiments began in situ. However, differences in frequencies of these subclades found between Birthday and Acer24 sites did not show differences between exact ITS2 subclades of *S. linucheae*. This suggests that site-specific environmental characteristics (i.e., high irradiance, higher temperature), not changes in *Symbiodinium* sp. subtypes, influenced stress on PSII that led to reduced quantum efficiencies.

Fragments within the 32 °C + LPS treatment had increases in both  $Fv'/Fm'$  and  $Fv/Fm$  ratios when compared to the 32 °C treatment and were comparable to 28 °C treatments in both  $Fv'/Fm'$  and  $Fv/Fm$  ratios. As such, our data suggest that the response to the immune system stimulant (i.e., LPS) may be indirectly beneficial to photosynthetic processes when combined with thermal stress by increasing the magnitude of the coral host immune response, where coral host cells mitigate oxidative stress by producing antioxidants [58,59]. Regardless of bleaching status, cellular byproducts known as reactive oxygen species (ROS) are produced as Symbiodiniaceae are undergoing photosynthesis [55,57]. Under optimal conditions, ROS are produced at a manageable concentration and are involved in cell signaling, cellular defense, and apoptosis [55,60,61]. As energy associated with the photosynthetic process increases, via increased light or heat, ROS concentrations increase to a point where damage to the photosynthetic process occurs via degradation of the D1 protein [56,62]. In addition, high temperature disrupts the Calvin cycle and damages thylakoid membranes within PSII [62–64]. These disruptions cause reductions in photosynthetic activities and lead to the loss of algal symbionts within a coral host [27,58]. LPS is a MAMP that triggers immune responses within coral organisms [17,40]. Specifically, the melanin synthesis pathway, an immune pathway in coral organisms, is known to generate antioxidants to reduce negative effects of pathogenic infection by triggering from MAMPs [17]. Antioxidants are an important suppressant to combat the negative effects of ROS toxicity and reduce overall oxidative stress [55,65]. A previous study [40] found significantly higher  $H_2O_2$  scavenging rates (i.e., antioxidants) in *Porites astreoides* from elevated temperature (32 °C) and LPS exposure treatments compared to elevated temperatures only. We propose that LPS is an important catalyst for increasing antioxidant concentrations to benefit bleaching susceptibility and oxidative stress. Our results suggest the coral host actively helps mitigate ROS toxicity by means of antioxidant production in translocated fragments from the Acer24 reef site, as hypothesized in other studies [66].

This research is a continuation of previously published work [32,36,37,67,68] on *Porites astreoides* from the Florida Keys. The collective results from these studies show the implications of site-based characteristics being influential on the physiology of these colonies. The offshore site (Acer24) was categorized as a non-stable, high-irradiance site not capable of recovery periods to mitigate environmental stressors. This site resulted in smaller colonies with less dense populations compared to inshore sites (Birthday Reef), likely due to Acer24 having higher expressions of immune-related genes (inflammatory and cellular stress based) compared to Birthday Reef, exhausting energy resources toward immune responses [67]. Similarly, we see a trend in these results that show Acer24 Reef having significantly lower photosynthetic efficiencies when exposed to higher temperatures in laboratory experiments compared to Birthday reef colonies. Our previous studies [67,68] indicate higher expressions of coral immune-related gene expressions, respectfully, from Acer24 colonies compared to Birthday Reef colonies from laboratory-based experiments. We postulate from these results that stress events exacerbate negative long-term physiological impacts from colonies native and/or translocated to the Acer24 Reef site.

## 5. Conclusions

In this study, we observed translocation effects, impacts of thermal stress, and plausible benefits of immune stimulant exposure on the photosynthetic efficiencies ( $Fv'/Fm'$  and  $Fv/Fm$ ) in *Porites astreoides* colonies from the lower Florida Keys. Climate change is an existential threat to corals worldwide, and we propose exacerbated stress from simulated thermal stress based on our results. In support from previous experiments, we suggest

that site-specific characteristics were influential in reduction of photosynthetic efficiencies. Acer24 sites had considerably higher irradiance to Birthday Reef sites and lacked a recovery period over the winter, which postulates the susceptibility of BA colonies compared to AA colonies, as translocation to stressful sites from non-stressful ones can reduce physiological plasticity. The increased irradiance from the Acer24 site implies higher ROS concentrations, causing further stress and degradation of photosynthetic components. Surprisingly, we observed significant increases in photosynthetic efficiencies when exposed to an immune stimulant (i.e., LPS) which were comparable to control treatment efficiencies (i.e., 28 °C). We propose that antioxidants generated from this immune stimulant was the primary cause of these significantly higher efficiencies, as antioxidants are the primary combatant against oxidative stress and H<sub>2</sub>O<sub>2</sub> scavenging has been shown to increase in *P. astreoides* when exposed to these particular stimulants. We propose that thermal stress alone degrades photosynthetic efficiency due to high concentrations of ROS and reduced concentrations of antioxidants. While these are strictly laboratory experiments run for a short period (8 h), disease could be considered a benefit to increase photosynthetic efficiencies based on our results. However, immune responses are extremely complex and future studies should incorporate in situ measurements on diseased coral colonies to further understand the total holobiont response in these conditions.

**Author Contributions:** Conceptualization, B.H.-S., J.A.H., J.M.C. and K.B.S.; methodology, B.H.-S., J.A.H. and K.B.S.; software, T.E.H. and J.A.H.; validation, B.H.-S., J.A.H. and K.B.S.; formal analysis, T.E.H. and J.A.H.; investigation, B.H.-S., J.A.H., J.M.C. and K.B.S.; resources, B.H.-S., J.A.H., J.M.C. and K.B.S.; data curation, T.E.H. and B.H.-S.; writing—original draft preparation, T.E.H. and B.H.-S.; writing—review and editing, T.E.H., B.H.-S., J.A.H., J.M.C. and K.B.S.; visualization, T.E.H.; supervision, B.H.-S. and K.B.S.; project administration, B.H.-S., J.A.H. and K.B.S.; funding acquisition, B.H.-S., J.A.H. and K.B.S. All authors have read and agreed to the published version of the manuscript.

**Funding:** We thank the Annis Water Resources Institute for both a graduate fellowship and research funding associated with this project, and Grand Valley State University for a Presidential Research Grant. We also thank Michigan State University RTSF and the Integrative Biology Department at Michigan State University (Graduate Fellowship), and the Coastal Preservation Network (Award 250542) for additional funding opportunities.

**Institutional Review Board Statement:** Not applicable.

**Informed Consent Statement:** Not applicable.

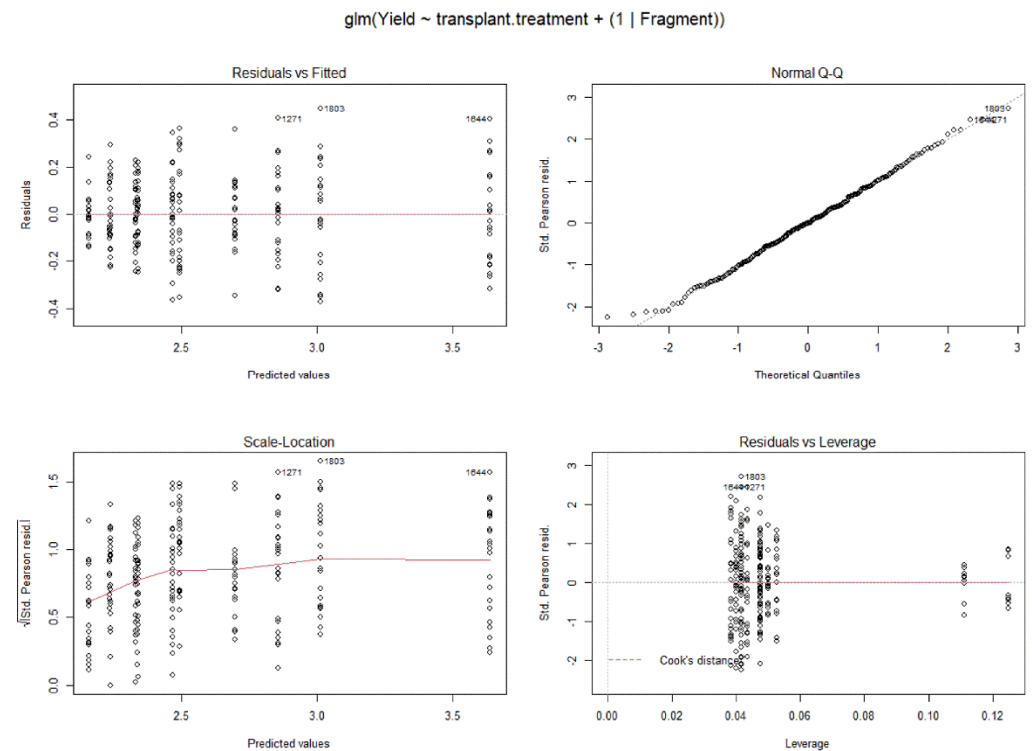
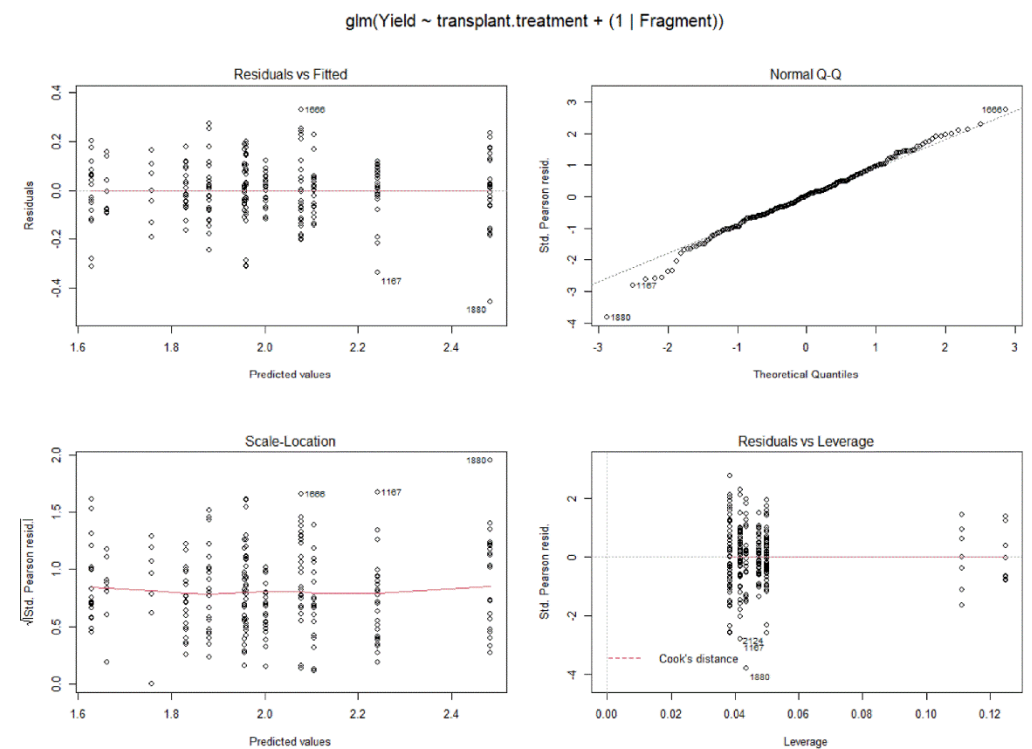
**Data Availability Statement:** The data that support the findings of this study are openly available in Water\_PAM\_Data repository at [github.com/teharman/Water\\_PAM\\_Data](https://github.com/teharman/Water_PAM_Data).

**Acknowledgments:** The authors acknowledge Eric Bartels and the Mote Marine Laboratory Staff for their help in the field and laboratory. In addition, we thank the Florida Keys National Marine Sanctuary for providing the permit for allowing this research to take place (permit number: FKNMS-2011-10). The authors also wish to express their gratitude to the editor and reviewers for their valuable comments and assistance in the revision of this manuscript.

**Conflicts of Interest:** The authors declare no conflict of interest.



## Appendix A

Figure A1. Model plots of effective quantum yield data in *Porites astreoides*.Figure A2. Model plots of maximum quantum yield data in *Porites astreoides*.

**Table A1.** Generalized mixed linear model results between fixed effects of translocation and treatment against a random effect of fragment number regarding effective quantum yield in *Porites astreoides* ( $Fv'/Fm'$ ). All bolded and highlighted  $p$ -values are considered significant ( $p \leq 0.05$ ).

	Estimate	Std. Error	t Value	Pr (>  t )
(Intercept)	2.16136	0.13455	16.063	<b>2.00E-16</b>
Acer24 to Acer24.32 °C	0.69441	0.20253	3.429	<b>0.0007</b>
Acer24 to Acer24.32 °C + LPS	0.30682	0.18915	1.622	0.1062
Acer24 to Bday.28 °C	0.07381	0.25633	0.288	0.7736
Acer24 to Bday.32 °C	0.17664	0.25173	0.702	0.4836
Acer24 to Bday.32 °C + LPS	0.07967	0.19055	0.418	0.6763
Bday to Acer24.28 °C	0.85011	0.20716	4.104	<b>0.0001</b>
Bday to Acer24.32 °C	1.47639	0.22908	6.445	<b>6.76E-10</b>
Bday to Acer24.32 °C + LPS	0.33192	0.18804	1.765	0.0789
Bday to Bday.28 °C	0.16985	0.19344	0.878	0.3808
Bday to Bday.32 °C	0.53492	0.20525	2.606	<b>0.0098</b>
Bday to Bday.32 °C + LPS	0.17928	0.19895	0.901	0.3685
1   FragmentTRUE	NA	NA	NA	NA

**Table A2.** Generalized mixed linear model results between fixed effects of translocation and treatment against a random effect of fragment number regarding maximum quantum yield in *Porites astreoides* ( $Fv/Fm$ ). All bolded and highlighted  $p$ -values are considered significant ( $p \leq 0.05$ ).

	Estimate	Std. Error	t Value	Pr (>  t )
(Intercept)	2.10589	0.09575	21.993	<b>2.00E-16</b>
Acer24 to Acer24.32 °C	0.13682	0.13254	1.032	0.3030
Acer24 to Acer24.32 °C + LPS	−0.22421	0.12499	−1.794	0.0742
Acer24 to Bday.28 °C	−0.44417	0.15886	−2.796	<b>0.0056</b>
Acer24 to Bday.32 °C	−0.34692	0.15723	−2.206	<b>0.0283</b>
Acer24 to Bday.32 °C + LPS	−0.10313	0.13141	−0.785	0.4334
Bday to Acer24.28 °C	−0.14601	0.1245	−1.173	0.2421
Bday to Acer24.32 °C	0.37786	0.13922	2.714	<b>0.0071</b>
Bday to Acer24.32 °C + LPS	−0.02825	0.12681	−0.223	0.8239
Bday to Bday.28 °C	−0.47585	0.12415	−3.833	<b>0.0002</b>
Bday to Bday.32 °C	−0.14843	0.13185	−1.126	0.2614
Bday to Bday.32 °C + LPS	−0.27479	0.12747	−2.156	<b>0.0321</b>
1   FragmentTRUE	NA	NA	NA	NA

## References

- Arto, I.; Dietzenbacher, E. Drivers of the growth in global greenhouse gas emissions. *Environ. Sci. Technol.* **2014**, *48*, 5388–5394. [[CrossRef](#)] [[PubMed](#)]
- Althor, G.; Watson, J.E.; Fuller, R.A. Global mismatch between greenhouse gas emissions and the burden of climate change. *Sci. Rep.* **2016**, *6*, 20281. [[CrossRef](#)] [[PubMed](#)]
- Wijffels, S.; Roemmich, D.; Monselesan, D.; Church, J.; Gilson, J. Ocean temperatures chronicle the ongoing warming of Earth. *Nat. Clim. Chang.* **2016**, *6*, 116–118. [[CrossRef](#)]
- Richmond, R.H. Coral reefs: Present problems and future concerns resulting from anthropogenic disturbance. *Am. Zool.* **1993**, *33*, 524–536. [[CrossRef](#)]
- Yonge, C.M.; Nicholls, A.G. Studies on the physiology of corals. IV. The structure, distribution, and physiology of the zooxanthellae. *Sci. Rep. Great Barrier Reef Exped. 1928–29* **1931**, *1*, 135–176.
- Brodersen, K.E.; Lichtenberg, M.; Ralph, P.J.; Kuhl, M.; Wangpraseurt, D. Radiative energy budget reveals high photosynthetic efficiency in symbiont-bearing corals. *J. R. Soc. Interface* **2014**, *11*, 20130997. [[CrossRef](#)]
- Mucsatine, L.; Porter, J.W. Reef corals: Mutualistic symbioses adapted to nutrient-poor environments. *BioScience* **1977**, *27*, 454–460.
- Roth, M.S. The engine of the reef: Photobiology of the coral-algal symbiosis. *Front. Microbiol.* **2014**, *5*, 422. [[CrossRef](#)]
- Lesser, M.P. Coral Bleaching: Causes and Mechanisms. In *Coral Reefs: An Ecosystem in Transition*; Dubinsky, Z., Stambler, N., Eds.; Springer: Dordrecht, The Netherlands, 2011; pp. 405–419.
- Eakin, C.M.; Morgan, J.A.; Heron, S.F.; Smith, T.B.; Liu, G.; Alvarez-Filip, L.; Baca, B.; Bartels, E.; Bastidas, C.; Bouchon, C.; et al. Caribbean corals in crisis: Record thermal stress, bleaching, and mortality in 2005. *PLoS ONE* **2010**, *5*, e13969. [[CrossRef](#)]

11. Moore, J.A.; Bellchambers, L.M.; Depczynski, M.R.; Evans, R.D.; Evans, S.N.; Field, S.N.; Friedman, K.J.; Gilmour, J.P.; Holmes, T.H.; Middlebrook, R.; et al. Unprecedented mass bleaching and loss of coral across 12 degrees of latitude in western Australia in 2010–11. *PLoS ONE* **2012**, *7*, e51807. [\[CrossRef\]](#)
12. Cervino, J.M.; Thompson, F.L.; Gomez-Gil, B.; Lorence, E.A.; Goreau, T.J.; Hayes, R.L.; Winiarski-Cervino, K.B.; Smith, G.W.; Huguen, K.; Bartels, E. The *Vibrio* core group induces yellow band disease in Caribbean and Indo-Pacific reef-building corals. *J. Appl. Microbiol.* **2008**, *105*, 1658–1671. [\[CrossRef\]](#) [\[PubMed\]](#)
13. Gignoux-Wolfsohn, S.A.; Marks, C.J.; Vollmer, S.V. White band disease transmission in the threatened coral, *Acropora cervicornis*. *Sci. Rep.* **2012**, *2*, 804. [\[CrossRef\]](#) [\[PubMed\]](#)
14. Aeby, G.S.; Ushijima, B.; Campbell, J.E.; Jones, S.; Williams, G.J.; Meyer, J.L.; Häse, C.; Paul, V.J. Pathogenesis of a tissue loss disease affecting multiple species of corals along the Florida reef tract. *Front. Mar. Sci.* **2019**, *6*, 678. [\[CrossRef\]](#)
15. Cervino, J.M.; Hayes, R.; Goreau, T.J.; Smith, G.W. Zooxanthellae regulation in yellow blotch/band and other coral diseases contrasted with temperature related bleaching: In situ destruction vs. expulsion. *Symbiosis* **2004**, *37*, 63–85.
16. Cervino, J.M.; Hayes, R.L.; Polson, S.W.; Polson, S.C.; Goreau, T.J.; Martinez, R.J.; Smith, G.W. Relationship of *Vibrio* species infection and elevated temperatures to yellow blotch/band disease in Caribbean corals. *Appl. Environ. Microbiol.* **2004**, *70*, 6855–6864. [\[CrossRef\]](#)
17. Palmer, C.V.; Traylor-Knowles, N. Towards an integrated network of coral immune mechanisms. *Proc. Biol. Sci.* **2012**, *279*, 4106–4114. [\[CrossRef\]](#)
18. Connelly, M.T.; McRae, C.J.; Liu, P.J.; Traylor-Knowles, N. Lipopolysaccharide treatment stimulates *Pocillopora* coral genotype-specific immune responses but does not alter coral-associated bacteria communities. *Dev. Comp. Immunol.* **2020**, *109*, 103717. [\[CrossRef\]](#)
19. Mydlarz, L.D.; McGinty, E.S.; Harvell, C.D. What are the physiological and immunological responses of coral to climate warming and disease? *J. Exp. Biol.* **2010**, *213*, 934–945. [\[CrossRef\]](#)
20. Mansfield, K.M.; Gilmore, T.D. Innate immunity and cnidarian-Symbiodiniaceae mutualism. *Dev. Comp. Immunol.* **2019**, *90*, 199–209. [\[CrossRef\]](#)
21. Kvennefors, E.C.; Leggat, W.; Kerr, C.C.; Ainsworth, T.D.; Hoegh-Guldberg, O.; Barnes, A.C. Analysis of evolutionarily conserved innate immune components in coral links immunity and symbiosis. *Dev. Comp. Immunol.* **2010**, *34*, 1219–1229. [\[CrossRef\]](#)
22. Palmer, C.V.; Bythell, J.C.; Willis, B.L. Levels of immunity parameters underpin bleaching and disease susceptibility of reef corals. *FASEB J.* **2010**, *24*, 1935–1946. [\[CrossRef\]](#) [\[PubMed\]](#)
23. Reed, K.C.; Muller, E.M.; van Woesik, R. Coral immunology and resistance to disease. *Dis. Aquat. Organ.* **2010**, *90*, 85–92. [\[CrossRef\]](#) [\[PubMed\]](#)
24. van de Water, J.; Chaib De Mares, M.; Dixon, G.B.; Raina, J.B.; Willis, B.L.; Bourne, D.G.; van Oppen, M.J.H. Antimicrobial and stress responses to increased temperature and bacterial pathogen challenge in the holobiont of a reef-building coral. *Mol. Ecol.* **2018**, *27*, 1065–1080. [\[CrossRef\]](#)
25. Young, B.D.; Serrano, X.M.; Rosales, S.M.; Miller, M.W.; Williams, D.; Traylor-Knowles, N. Innate immune gene expression in *Acropora palmata* is consistent despite variance in yearly disease events. *PLoS ONE* **2020**, *15*, e0228514. [\[CrossRef\]](#)
26. Burns, J.H.; Gregg, T.M.; Takabayashi, M. Does coral disease affect symbiodinium? Investigating the impacts of growth anomaly on symbiont photophysiology. *PLoS ONE* **2013**, *8*, e72466. [\[CrossRef\]](#) [\[PubMed\]](#)
27. Krueger, T.; Hawkins, T.D.; Becker, S.; Pontasch, S.; Dove, S.; Hoegh-Guldberg, O.; Leggat, W.; Fisher, P.L.; Davy, S.K. Differential coral bleaching contrasting the activity and response of enzymatic antioxidants in symbiotic partners under thermal stress. *Comp. Biochem. Physiol. A. Mol. Integr. Physiol.* **2015**, *190*, 15–25. [\[CrossRef\]](#) [\[PubMed\]](#)
28. Barshis, D.J.; Ladner, J.T.; Oliver, T.A.; Seneca, F.O.; Traylor-Knowles, N.; Palumbi, S.R. Genomic basis for coral resilience to climate change. *Proc. Natl. Acad. Sci. USA* **2013**, *110*, 1387–1392. [\[CrossRef\]](#)
29. Palumbi, S.R.; Barshis, D.J.; Traylor-Knowles, N.; Bay, R.A. Mechanisms of reef coral resistance to future climate change. *Science* **2014**, *344*, 895–898. [\[CrossRef\]](#)
30. Barshis, D.J.; Ladner, J.T.; Oliver, T.A.; Palumbi, S.R. Lineage-specific transcriptional profiles of *Symbiodinium* spp. unaltered by heat stress in a coral host. *Mol. Biol. Evol.* **2014**, *31*, 1343–1352. [\[CrossRef\]](#)
31. Klepac, C.N.; Barshis, D.J. Reduced thermal tolerance of massive coral species in a highly variable environment. *Proc. Biol. Sci.* **2020**, *287*, 20201379. [\[CrossRef\]](#)
32. Salas, B.H.; Haslun, J.A.; Strychar, K.B.; Ostrom, P.H.; Cervino, J.M. Site-specific variation in gene expression from *Symbiodinium* spp. associated with offshore and inshore *Porites astreoides* in the lower Florida Keys is lost with bleaching and disease stress. *PLoS ONE* **2017**, *12*, e0173350. [\[CrossRef\]](#) [\[PubMed\]](#)
33. Jin, Y.K.; Lundgren, P.; Lutz, A.; Raina, J.B.; Howells, E.J.; Paley, S.A.; Willis, B.L.; van Oppen, M.J.H. Genetic markers for antioxidant capacity in a reef-building coral. *Sci. Adv.* **2016**, *2*, e1500842. [\[CrossRef\]](#) [\[PubMed\]](#)
34. Drury, C.; Lirman, D. Genotype by environment interactions in coral bleaching. *Proc. Biol. Sci.* **2021**, *288*, 20210177. [\[CrossRef\]](#) [\[PubMed\]](#)
35. Barott, K.L.; Huffmyer, A.S.; Davidson, J.M.; Lenz, E.A.; Matsuda, S.B.; Hancock, J.R.; Innis, T.; Drury, C.; Putnam, H.M.; Gates, R.D. Coral bleaching response is unaltered following acclimatization to reefs with distinct environmental conditions. *Proc. Natl. Acad. Sci. USA* **2021**, *118*, e2025435118. [\[CrossRef\]](#)

36. Hauff, B.; Haslun, J.A.; Strychar, K.B.; Ostrom, P.H.; Cervino, J.M. Symbiont diversity of zooxanthellae (*Symbiodinium* spp.) in *Porites astreoides* and *Montastraea cavernosa* from a reciprocal transplant in the lower Florida Keys. *Int. J. Biol.* **2016**, *8*, 9–22. [\[CrossRef\]](#)
37. Haslun, J.; Hauff, B.; Strychar, K.; Cervino, J. Decoupled seasonal stress as an indication of chronic stress in *Montastraea cavernosa* and *Porites astreoides* inhabiting the Florida reef tract. *Int. J. Mar. Sci.* **2016**, *6*, 1–20. [\[CrossRef\]](#)
38. Bhagooli, R.; Hidaka, M. Photoinhibition, bleaching susceptibility and mortality in two scleractinian corals, *Platygyra ryukyuensis* and *Stylophora pistillata*, in response to thermal and light stresses. *Comp. Biochem. Physiol. A Mol. Integr. Physiol.* **2003**, *137*, 547–555. [\[CrossRef\]](#)
39. Silverstein, R.N.; Cuning, R.; Baker, A.C. Tenacious D: *Symbiodinium* in clade D remain in reef corals at both high and low temperature extremes despite impairment. *J. Exp. Biol.* **2017**, *220*, 1192–1196. [\[CrossRef\]](#)
40. Palmer, C.V.; McGinty, E.S.; Cummings, D.J.; Smith, S.M.; Bartels, E.; Mydlarz, L.D. Patterns of coral ecological immunology: Variation in the responses of Caribbean corals to elevated temperature and a pathogen elicitor. *J. Exp. Biol.* **2011**, *214*, 4240–4249. [\[CrossRef\]](#)
41. Maxwell, K.; Johnson, G.N. Chlorophyll fluorescence—A practical guide. *J. Exp. Bot.* **2000**, *51*, 659–668. [\[CrossRef\]](#)
42. RStudio Team. *RStudio: Integrated Development for R*; RStudio: Boston, MA, USA, 2021.
43. R Core Team. *R: A Language and Environment for Statistical Computing*; R Foundation for Statistical Computing: Vienna, Austria, 2021.
44. Lenth, R.V. Least-Squares Means: The R Package lsmeans. *J. Stat. Softw.* **2016**, *69*, 1–33. [\[CrossRef\]](#)
45. Ware, M.; Garfield, E.N.; Nedimyer, K.; Levy, J.; Kaufman, L.; Precht, W.; Winters, R.S.; Miller, S.L. Survivorship and growth in staghorn coral (*Acropora cervicornis*) outplanting projects in the Florida Keys National Marine Sanctuary. *PLoS ONE* **2020**, *15*, e0231817. [\[CrossRef\]](#) [\[PubMed\]](#)
46. Muller, E.M.; Bartels, E.; Baums, I.B. Bleaching causes loss of disease resistance within the threatened coral species *Acropora cervicornis*. *eLife* **2018**, *7*, e35066. [\[CrossRef\]](#) [\[PubMed\]](#)
47. Downs, C.A.; McDougall, K.E.; Woodley, C.M.; Fauth, J.E.; Richmond, R.H.; Kushmaro, A.; Gibb, S.W.; Loya, Y.; Ostrander, G.K.; Kramarsky-Winter, E. Heat-stress and light-stress induce different cellular pathologies in the symbiotic dinoflagellate during coral bleaching. *PLoS ONE* **2013**, *8*, e77173. [\[CrossRef\]](#)
48. Jimenez, I.M.; Kuhl, M.; Larkum, A.W.D.; Ralph, P.J. Heat budget and thermal microenvironment of shallow-water corals: Do massive corals get warmer than branching corals? *Limnol. Oceanogr.* **2008**, *53*, 1548–1561. [\[CrossRef\]](#)
49. Jimenez, I.M.; Kuhl, M.; Larkum, A.W.; Ralph, P.J. Effects of flow and colony morphology on the thermal boundary layer of corals. *J. R. Soc. Interface* **2011**, *8*, 1785–1795. [\[CrossRef\]](#)
50. Falkowski, P.G.; Dubinsky, Z. Light-shade adaptation of *Stylophora pistillata*, a hermatypic coral from the Gulf of Eilat. *Nature* **1981**, *289*, 172–174. [\[CrossRef\]](#)
51. Dove, S.G.; Lovell, C.; Fine, M.; Deckenback, J.; Hoegh-Guldberg, O.; Iglesias-Prieto, R.; Anthony, K.R. Host pigments: Potential facilitators of photosynthesis in coral symbioses. *Plant Cell Environ.* **2008**, *31*, 1523–1533. [\[CrossRef\]](#)
52. Smith, E.G.; D'Angelo, C.; Salih, A.; Wiedenmann, J. Screening by coral green fluorescent protein (GFP)-like chromoproteins supports a role in photoprotection of zooxanthellae. *Coral Reefs* **2013**, *32*, 463–474. [\[CrossRef\]](#)
53. Ralph, P.J.; Larkum, A.W.D.; Kuhl, M. Temporal patterns in effective quantum yield of individual zooxanthellae expelled during bleaching. *J. Exp. Mar. Biol. Ecol.* **2005**, *316*, 17–28. [\[CrossRef\]](#)
54. Downs, C.A.; Fauth, J.E.; Halas, J.C.; Dustan, P.; Bemiss, J.; Woodley, C.M. Oxidative stress and seasonal coral bleaching. *Free Radic. Biol. Med.* **2002**, *33*, 533–543. [\[CrossRef\]](#)
55. McGinty, E.S.; Pieczonka, J.; Mydlarz, L.D. Variations in reactive oxygen release and antioxidant activity in multiple *Symbiodinium* types in response to elevated temperature. *Microb. Ecol.* **2012**, *64*, 1000–1007. [\[CrossRef\]](#) [\[PubMed\]](#)
56. Roberty, S.; Furla, P.; Plumier, J.C. Differential antioxidant response between two *Symbiodinium* species from contrasting environments. *Plant Cell Environ.* **2016**, *39*, 2713–2724. [\[CrossRef\]](#) [\[PubMed\]](#)
57. Nielsen, D.A.; Petrou, K.; Gates, R.D. Coral bleaching from a single cell perspective. *ISME J.* **2018**, *12*, 1558–1567. [\[CrossRef\]](#) [\[PubMed\]](#)
58. Richier, S.; Furla, P.; Plantivaux, A.; Merle, P.L.; Allemand, D. Symbiosis-induced adaptation to oxidative stress. *J. Exp. Biol.* **2004**, *208 Pt 2*, 277–285. [\[CrossRef\]](#)
59. Gardner, S.G.; Raina, J.B.; Nitschke, M.R.; Nielsen, D.A.; Stat, M.; Motti, C.A.; Ralph, P.J.; Petrou, K. A multi-trait systems approach reveals a response cascade to bleaching in corals. *BMC Biol.* **2017**, *15*, 117. [\[CrossRef\]](#)
60. Edreva, A. Generation and scavenging of reactive oxygen species in chloroplasts: A submolecular approach. *Agric. Ecosyst. Environ.* **2005**, *106*, 119–133. [\[CrossRef\]](#)
61. Kristiansen, K.A.; Jensen, P.E.; Moller, I.M.; Schulz, A. Monitoring reactive oxygen species formation and localization in living cells by use of the fluorescent probe CM-H<sub>2</sub>DCFDA and confocal laser microscopy. *Physiol. Plant* **2009**, *136*, 369–383. [\[CrossRef\]](#)
62. Lesser, M.P. Phylogenetic signature of light and thermal stress for the endosymbiotic dinoflagellates of corals (Family Symbiodiniaceae). *Limnol. Oceanogr.* **2019**, *64*, 1852–1863. [\[CrossRef\]](#)
63. Tchernov, D.; Gorbunov, M.Y.; de Vargas, C.; Yadav, S.N.; Milligan, A.J.; Hagglblom, M.; Falkowski, P.G. Membrane lipids of symbiotic algae are diagnostic of sensitivity to thermal bleaching in corals. *Proc. Natl. Acad. Sci. USA* **2004**, *101*, 13531–13535. [\[CrossRef\]](#)



- 
64. Wietherger, A.; Starzak, D.E.; Gould, K.S.; Davy, S.K. Differential ROS generation in response to stress in *Symbiodinium* spp. *Biol. Bull.* **2018**, *234*, 11–21. [[CrossRef](#)] [[PubMed](#)]
  65. Ayalon, I.; de Barros Marangoni, L.F.; Benichou, J.I.C.; Avisar, D.; Levy, O. Red Sea corals under artificial light pollution at night (ALAN) undergo oxidative stress and photosynthetic impairment. *Glob. Chang. Biol.* **2019**, *25*, 4194–4207. [[CrossRef](#)] [[PubMed](#)]
  66. Baird, A.H.; Bhagooli, R.; Ralph, P.J.; Takahashi, S. Coral bleaching: The role of the host. *Trends Ecol. Evol.* **2009**, *24*, 16–20. [[CrossRef](#)] [[PubMed](#)]
  67. Haslun, J.A.; Salas, B.H.; Strychar, K.B.; Ostrom, N.E.; Cervino, J.M. Biotic stress contributes to seawater temperature induced stress in a site-specific manner for *Porites astreoides*. *Mar. Biol.* **2018**, *165*, 160. [[CrossRef](#)]
  68. Haslun, J.A.; Salas, B.H.; Strychar, K.B.; Cervino, J.M.; Ostrom, N.E. Variation in immune-related gene expression provides evidence of local adaptation in *Porites astreoides* (Lamarck, 1816) between inshore and offshore meta-populations inhabiting the lower Florida reef tract, USA. *Water* **2021**, *13*, 2107. [[CrossRef](#)]